JOURNAL OF CATALYSIS 117, 78–90 (1989)

Evolution of Bimodal Distributions in the Sintering of Model Supported Metal Catalysts

AKSHAY BELLARE,* DADY B. DADYBURJOR,* AND MICHAEL J. KELLEY†

*Department of Chemical Engineering, West Virginia University, Morgantown, West Virginia 26506-6101; and †Engineering Technology Laboratory, Experimental Station, E. I. du Pont de Nemours & Company, Incorporated, Wilmington, Delaware 19880-0304

Received May 2, 1988; revised November 30, 1988

Model $Pt/\gamma\text{-}Al_2O_3$ catalysts were prepared and characterized in our laboratories. They were sintered in flowing oxygen at 600°C for up to 24 h. Particle sizes, shapes, and relative positions were determined from bright field images, and crystal structures from diffraction in the transmission electron microscope. Ion scattering spectroscopy gave surface compositions. The platinum particles in the unsintered samples were uniformly sized and evenly distributed upon the support. The sintered samples contained some larger particles, along with smaller (2-nm) particles that uniformly covered the support surface, giving rise to a bimodal size distribution. The average size of the particles in the larger mode increased with time, while both the size and the number of the particles in the smaller mode remained substantially constant. The average size of the larger particles after 24 h sintering was compared to a theoretical model that considers Ostwald ripening and particle migration. Agreement between the calculated and the observed distributions requires a lower than expected value for the metal–support interfacial tension. The value is consistent with the presence of metal oxide rather than metal in contact with the support. Surface analysis showed that at least the free surface of the metal particles is oxidized, while electron microscopy indicates that the interior remains as metal. This structure is also expected to affect the particle size distribution by promoting splitting until the entire particle is converted to oxide.

INTRODUCTION

Supported metal catalysts are used throughout petroleum and chemical processing industries under conditions ranging from mild, typical of selective hydrogenations, to severe, typical of emission abatement, with hydrocarbon conversions such as naptha reforming someplace in between. All catalysts deactivate and a number of mechanisms are known to operate. Under severe conditions, sintering is prominent, leading to a loss in activity via the loss of net metal surface area as particles grow larger.

Exposure to oxygen near 550°C is known to be effective for restoring the surface area of alumina-supported platinum and has been studied extensively (*1*). Direct observation of this redispersion by transmission electron microscopy (TEM) is greatly facilitated by using model catalysts. These consist of metal (here, platinum) applied to a transition alumina film generated on the surface of high-purity aluminum foil, removed before the electron microscopy (*2*). By this means, Ruckenstein and Malhotra (*3*) observed changes in the average platinum particle size after heating in air for 24 h at varying temperature. They qualitatively hypothesized the formation of a platinum–alumina complex that causes splitting of the particles. Gollob and Dadyburjor (*4*) studied the effect of air at 500°C on the particle size of similar catalysts for times up to 2 h. The observed particle splitting has been successfully incorporated into a mathematical model of redispersion (*5*).

In this work, sintering of platinum/alumina catalysts in flowing pure oxygen is studied for times up to 24 h. In addition to TEM images, a special effort was made to establish the composition and structure of these materials, including electron diffrac-

0021-9517/89 $3.00

tion, X-ray emission spectroscopy (XES), and ion scattering spectroscopy (ISS). Use of an extended range of TEM image magnifications reveals the existence of a bimodal distribution of particles. While the oxygen treatments lead to relatively little change in the size and number of the smaller particles, the larger end of the bimodal distribution shows an increase in the average particle size. A similar finding for platinum supported on high-surface-area alumina was reported previously (*6*). The present results are compared with a theoretical model for sintering of particles on a support. The next section presents the experimental work, followed by a discussion of the results in the final sections.

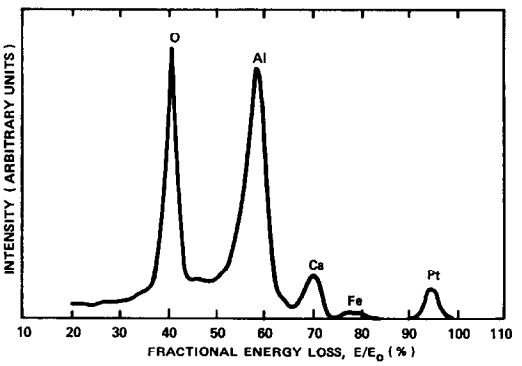

FIG. 1. ^{4}He ion scattering spectrum of model catalyst prior to treatment.

METHODS

The method used to prepare the model catalyst samples is based on that of Ruckenstein and Malhotra (*3*). The surface of high-purity aluminum foil is oxidized, heat-treated, and then sputter-coated with platinum; the platinum/alumina layer is removed from the underlying aluminum foil after sintering.

Aluminum foil, 0.1 mm thick (Puratronic, Aesar, Johnson Matthey), was cut into strips 40 by 15 mm. The strips were polished in a solution containing 100 ml of 85% (by weight) orthophosphoric acid, 4 ml of 70% (by weight) nitric acid, and 20 ml distilled water for a time of 3 min at 80°C followed by washing in distilled water. They were then oxidized in 150 ml distilled water containing 4.5 g of tartaric acid, maintained at pH 5.5 by addition of ammonium hydroxide. A current of 30 mA was passed for 20 s between the aluminum strip (anode) and a stainless-steel wire (cathode) under the control of a Keithley 220 programmable current source. The resulting oxide film was stabilized by heating in air at 600°C for 24 h, a treatment found in our previous work to yield γ-alumina.

Platinum was sputtered onto the alumina support using a Film-Vac EMS-76M sputtering unit. After evacuation, back-fill, and reevacuation, an argon bleed maintained chamber pressure at 200 μm Hg during sputtering. Potential backstreaming of hydrocarbon vapors from the pump into the sputtering chamber was eliminated by a molecular sieve trap manufactured by K. J. Lesker Co. An output current of 40 mA sufficed to yield platinum coverages near 1% after a few minutes.

All the catalyst specimens examined here were cut from a single original 15 × 40-mm sheet. They were subjected to oxygen (Linde UHP, 5A molecular sieve) flowing at 100 ml/min at 600°C for up to 24 h. The quartz reactor tubes were previously conditioned in the same oxygen flow for not less than 24 h at 750°C. The surface composition prior to sintering was examined by ion scattering spectroscopy, which uniquely offers first-monolayer analytical sensitivity. The spectrum in Fig. 1 was obtained with helium so that oxygen and aluminum as well as platinum could be observed. Small amounts of calcium and iron are also evident; however, published sensitivity factors (*7*) indicate that their concentrations are quite small, and we do not believe them to be a factor in the present results. We know of no other surface analyses of platinum/alumina model catalysts with which to compare them. Platinum was not seen in spectra taken from oxygen-treated samples.

For TEM studies, the film of platinum on alumina was stripped from the underlying foil by a saturated mercuric chloride solution and washed repeatedly in distilled water to minimize chloride contamination. TEM images and diffraction patterns were obtained in a Philips EM-420 TEM; local elemental analyses were obtained by X-ray emission spectroscopy in both the scanning transmission electron microscopy (STEM) and the normal modes in a twin-lens Philips EM-400 TEM. Figure 2 shows a typical X-ray spectrum; note that peaks from aluminum and copper (support grid) are off-scale to better reveal weaker emissions. A trace of iron is seen, but there is little evidence of either chlorine or mercury at the expected peak positions. On occasional grids there was a substantial chlorine peak, which we attribute to inadequate washing. Platinum was detected without regard to whether it was evident by ISS or not. All particles large enough for individual analysis by STEM/XES were platinum. Note that oxygen would not be seen since our microscope does not have a windowless X-ray detector. Electron diffraction indicates that the alumina films obtained after anodization and heat treatment were always the expected γ-alumina and had no strong orientation.

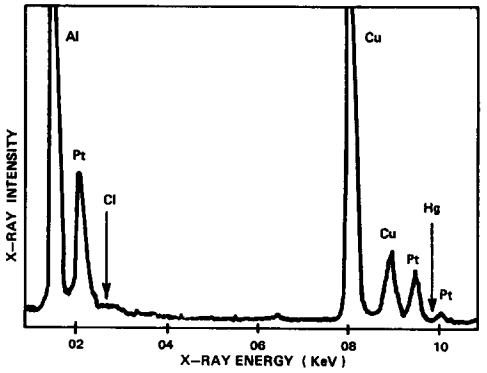

FIG. 2. X-ray emission spectrum of model catalyst after 6 h heating.

RESULTS

A series of TEM images illustrates the evolution of microstructure with sintering, beginning with an unsintered sample (Fig. 3). Here, uniformly sized platinum particles having an average diameter of 4 nm are distributed on the alumina surface. After 2 h at 600°C in flowing oxygen, a few large particles are evident (Fig. 4) in addition. After 3 h, the large particles increase in size and number (Fig. 5). They show facetting, while the small particles remain circular and retain their size, but are somewhat less numerous.

Six hours of heating brings about a further increase in the size of the large particles (Fig. 6) to a surface-area-averaged diameter of 20.9 nm. Examining this same field at higher magnification (Fig. 7) discloses a spatially uniform distribution of even smaller particles, about 2-nm average diameter compared to the 4-nm particles noted above. Relatively few such particles are seen at heating times of less than 6 h.

The general features after 24 h remain the same (Fig. 8). The larger particles grow to a surface-area-averaged diameter of 29.7 nm, and the smaller (2-nm) particles are again evident at high magnification (Fig. 9). This bimodal distribution is evident in the particle size measurements (Figs. 10a and 10b) taken under the unsintered and 6- and 24-h sintered conditions.

DISCUSSION

The results can be summarized as the development of a bimodal particle size distribution. The freshly prepared catalyst sample has uniformly sized and evenly distributed platinum particles on the alumina support. After 2 h in flowing oxygen at 600°C, an overall increase in the average particle size is seen, as expected. The distribution consists of some large particles, with many small ones. Three hours of heating brings a further increase in the size of the large particles. For a 6-h treatment, smaller-sized particles are seen to evolve, and these particles are unchanged in size and number even after 24 h of sintering.

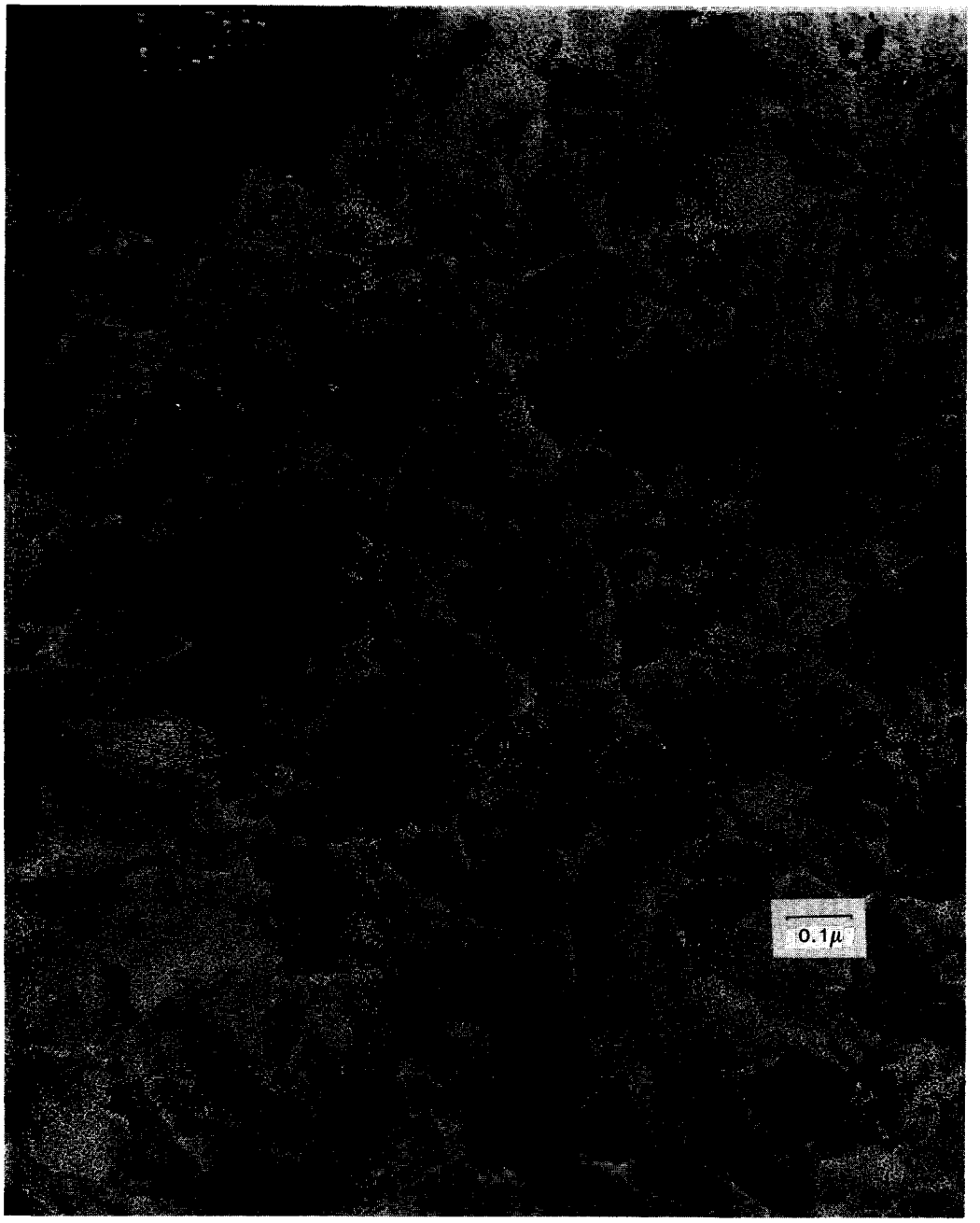

FIG. 3. Transmission electron microscope image of freshly prepared model Pt/aluminum catalyst. The particles are almost unisized at 4 nm.

Our understanding of these results is aided by a theoretical model presented by Bellare and Dadyburjor (*8*), extending previous work on Ostwald ripening of metal particles on a flat substrate (*9*). The present model incorporates the interaction of all particles with one another through the adatom field, rather than using a "mean field"

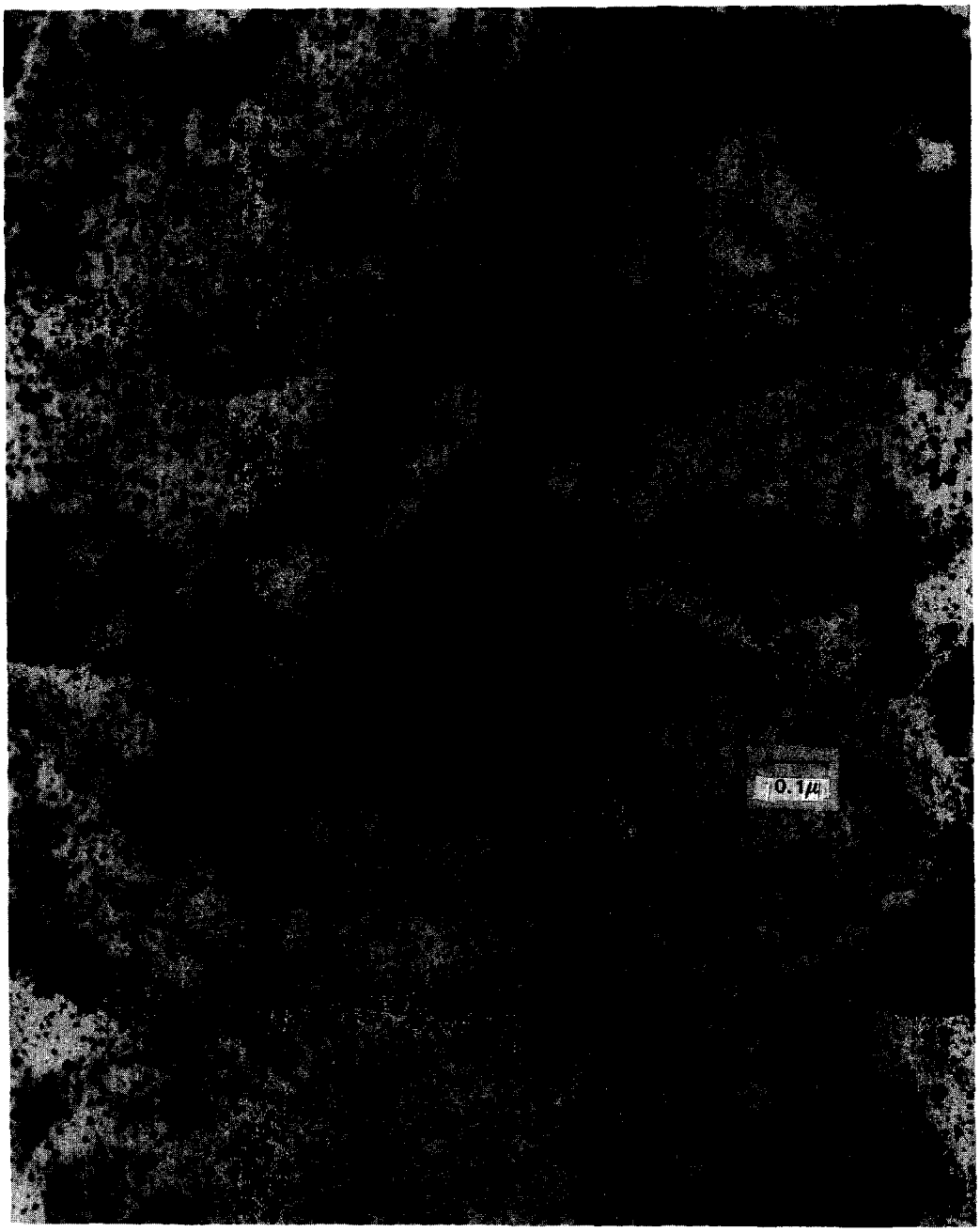

FIG. 4. TEM image after 2 h at 600°C in flowing oxygen. Several larger particles can be seen.

approach (*10*), and can account for both Ostwald ripening and particle migration. The sizes and locations of a representative sample of particles are required as the initial condition for the model, and data obtained from the sample heated for 6 h are used for this purpose. Since the particles in the smaller mode are unaltered in size and relative number up to a heating time of 24 h, and since the relative number of these "in-

FIG. 5. TEM image after 3 h at 600°C in flowing oxygen.

ert" particles (which do not increase in size) would flood that of the particles in the larger mode, only the latter particles are used for the initial data and for the calculations. The particle size distribution and average particle size calculated from the model can be compared with the experimental results at a heating time of 24 h.

Figure 11 plots the average particle radius $\bar{R}$ as a function of time for two values

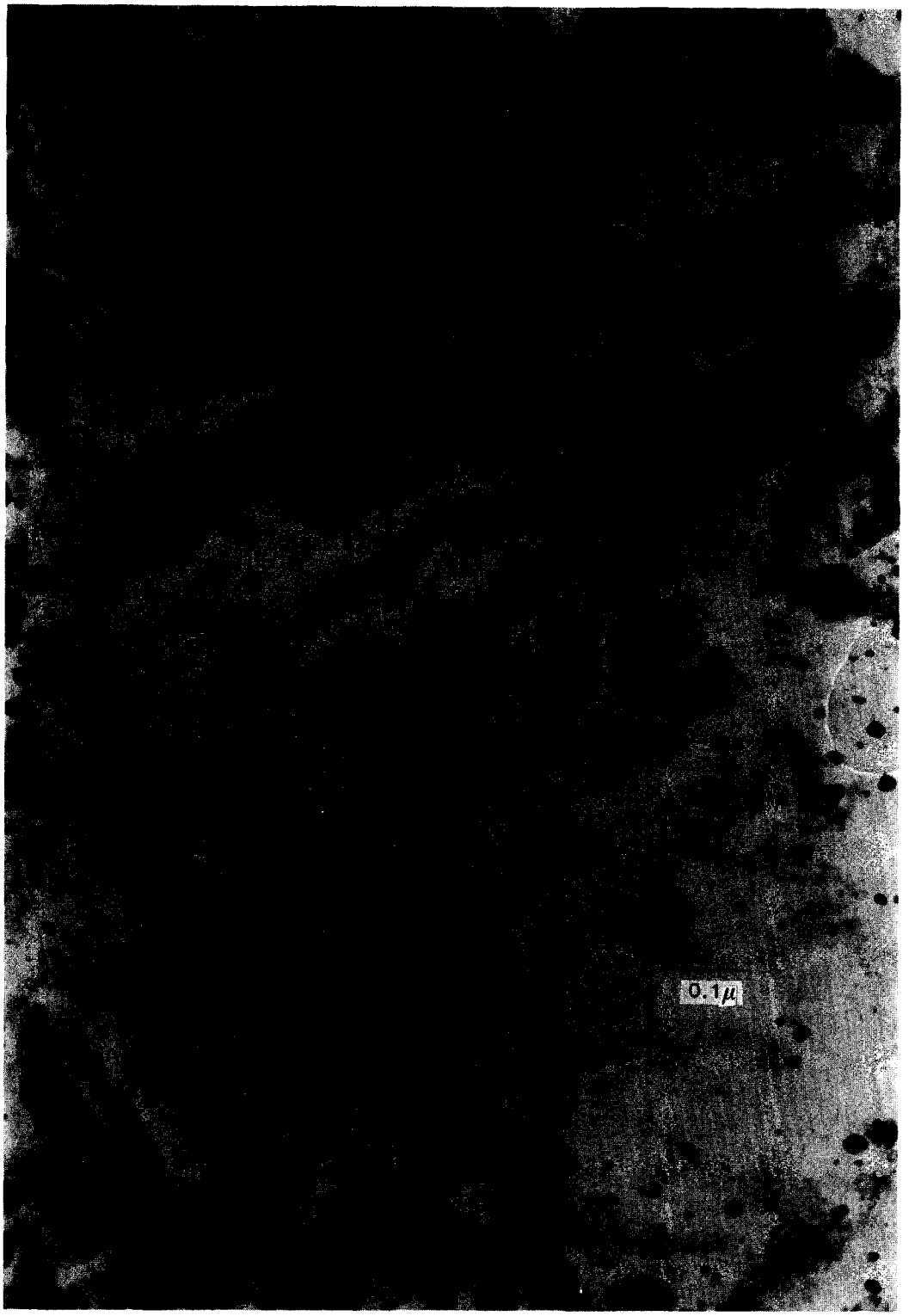

FIG. 6. TEM image after 6 h at 600°C in flowing oxygen. Very few particles of size comparable to the initial (4-nm) size can be seen.

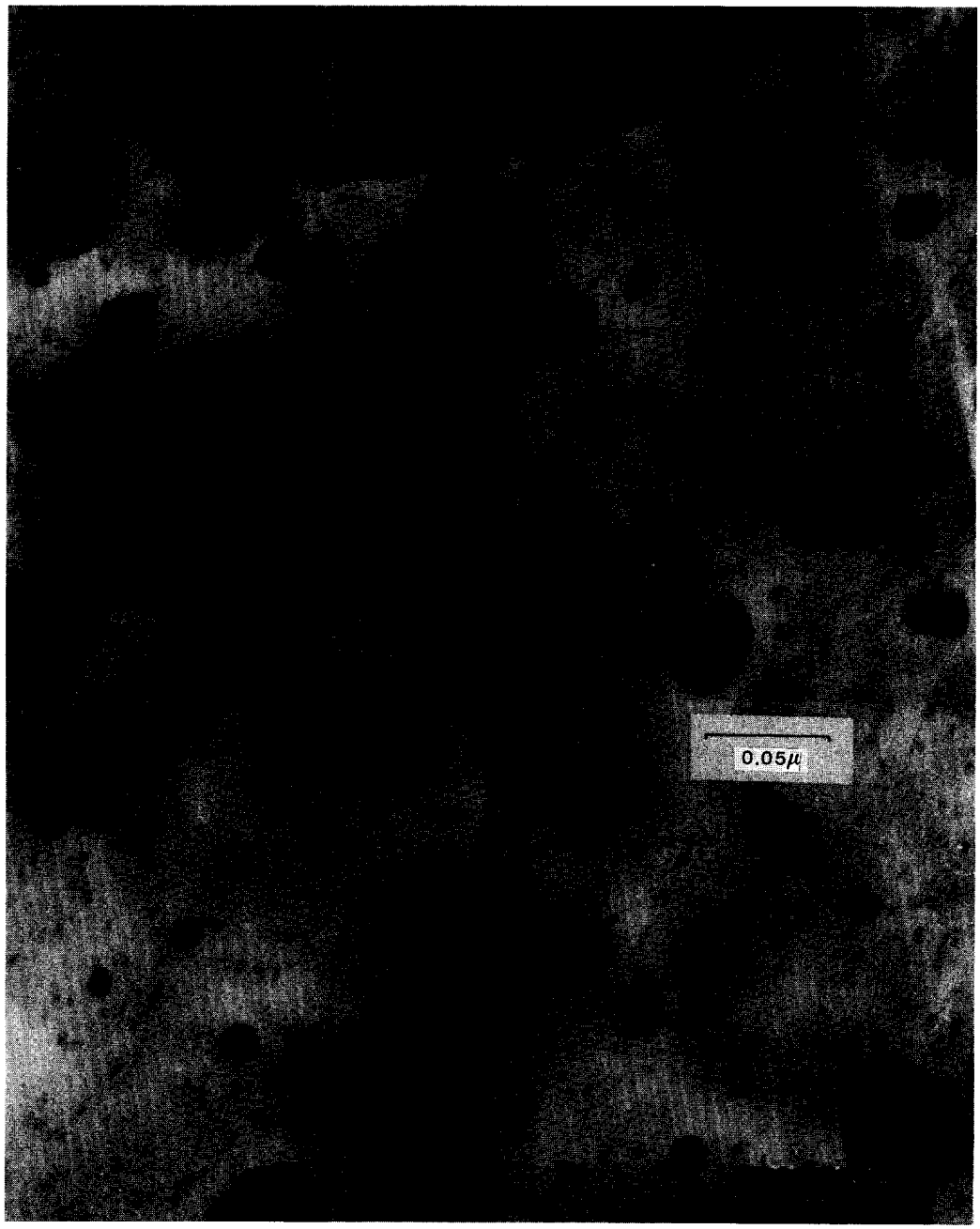

FIG. 7. Same sample as in Fig. 6, but at higher magnification. Along with the large particles can also be seen many particles smaller than the initial size (2 nm vs 4 nm).

of the model parameter l_c, the characteristic length [see Appendix: Nomenclature]. The parameter l_c arises from the Gibbs–Thomson equation

$$C_p = C_0 \exp[l_c/\bar{R}] \quad (1)$$

and is related to the interfacial tension between the particle and the support through

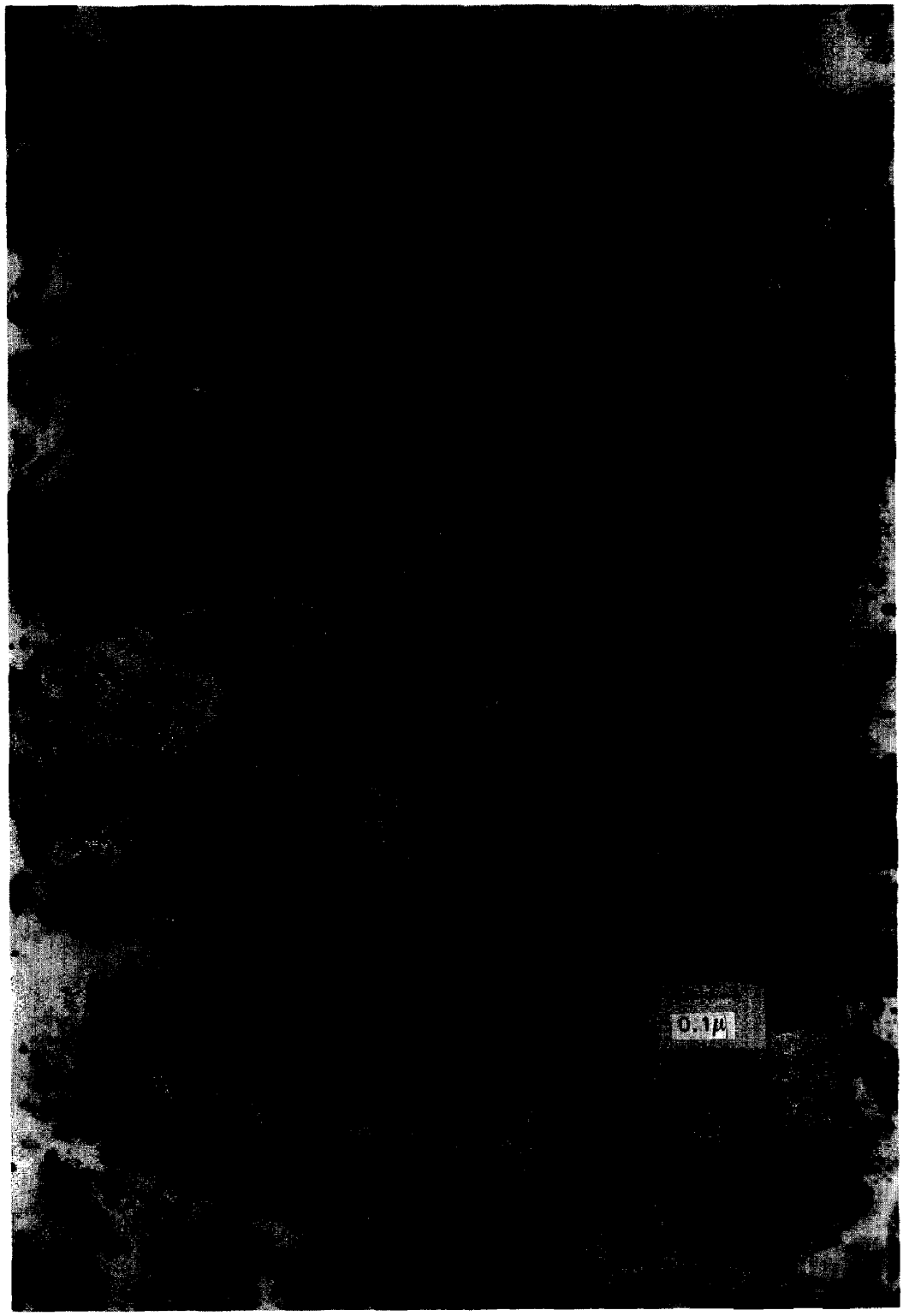

FIG. 8. TEM image after 24 h at 600°C in flowing oxygen.

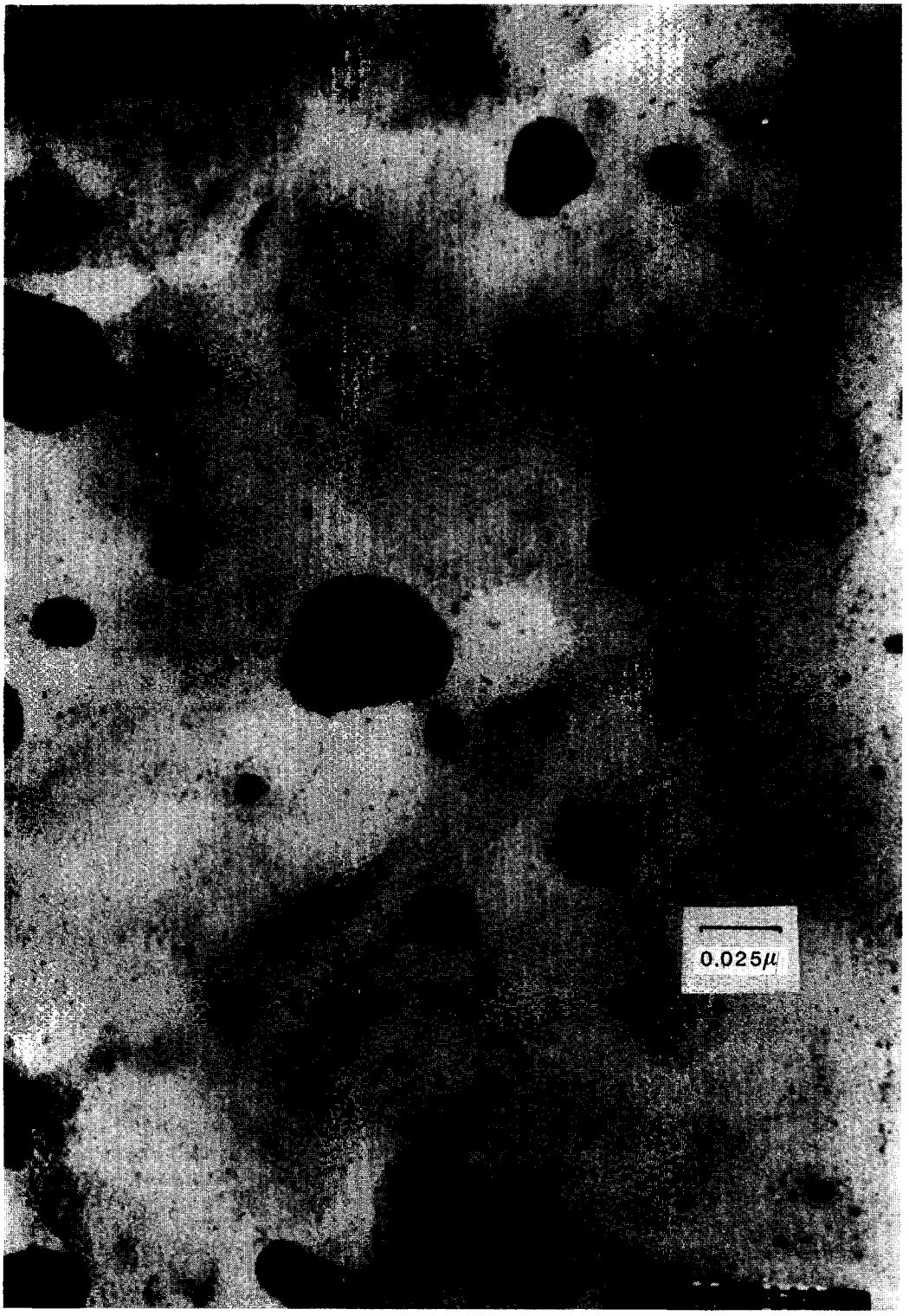

FIG. 9. Same sample as in Fig. 8, but at higher magnification. The smaller particles are qualitatively similar to those in Fig. 7 in number and size.

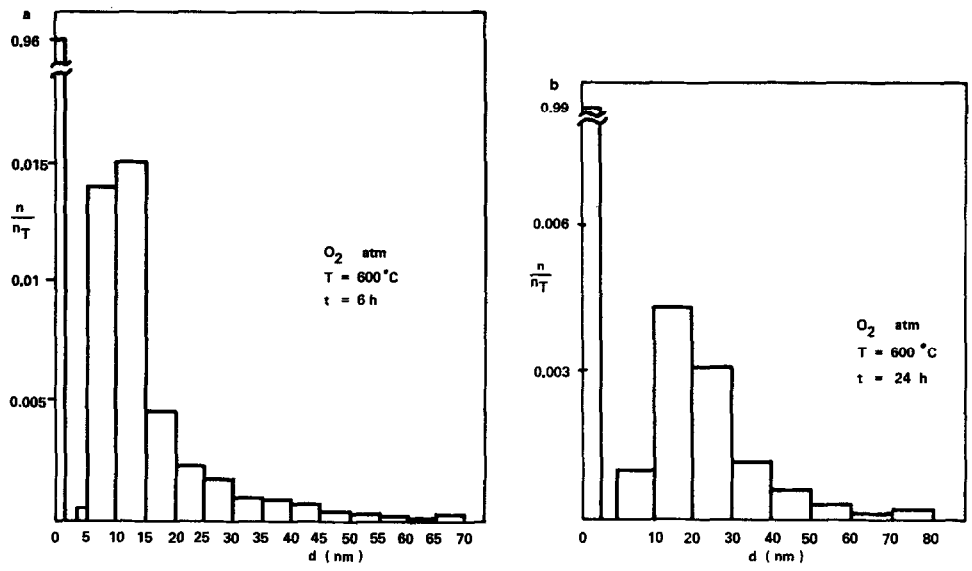

FIG. 10. Particle size distributions corresponding to (a) 6 h (Figs. 4 and 5), (b) 24 h (Figs. 6 and 7) in flowing oxygen.

the definition

$$l_c = 2\ V_m\ \sigma/kT. \qquad (2)$$

The value of 1.2 in Fig. 11 is considered a nominal value for this parameter for Pt/alumina systems (*8*) and the other value, 0.55, gives the best fit to the present results. Taken at face value, this indicates considerably lower particle–support interfacial tension here than in previous work. This would be expected if the metal particles were completely encapsulated by an oxide film, for example.

The particle size distribution obtained from the model calculations is shown in Fig. 12 and can be compared to that from the experimental micrographs in Fig. 10. Both distributions have similar relative shapes and the differences in the peak heights arise from the small differences in the relative number of the smaller particles. The calculated value for the number density of the smaller particles is obtained by assuming that the total number of the smaller particles is unaltered from the initial value. While this leads to a relative error of less than 1% in the calculated number density of the smaller particles, this difference is large enough to throw off the calculated number density of the larger particles, which are less numerous. However, the relative shape of the particle size distribution

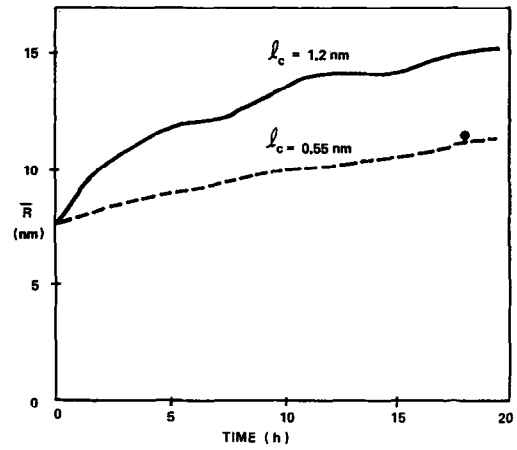

FIG. 11. Comparison of experimental and calculated change in surface-area-average radius $\bar{R}$ with sintering time. Initial particle sizes and locations for the calculations are obtained from experimental micrographs after 6 h heating. The solid curve uses the value of the characteristic length l_c from the previous study (*9*). The point represents the experimental value of $\bar{R}$ after 24 h heating (i.e., Δt = 18 h). The dashed curve is an approximate fit to the model by varying l_c. The resulting lower value (0.55 vs 1.2) implies increased particle–surface interaction.

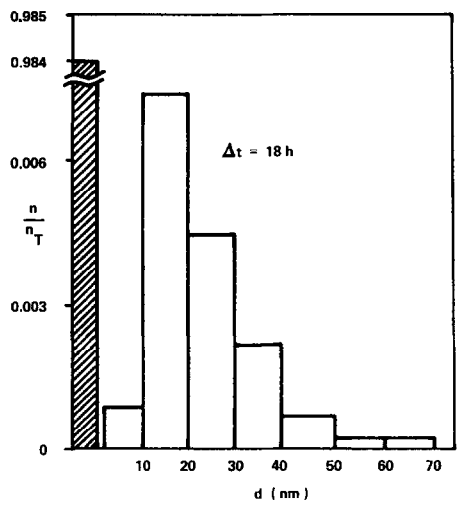

FIG. 12. Calculated size distribution corresponding to Δt = 18 h and l_c = 0.55 nm, i.e., the fitted curve of Fig. 11. The hatched portion of the histograph is obtained by noting that the small (2-nm) particles do not change in number or size beyond 6 h.

for the larger particles is similar to that of the experimental distribution. (If particles in the smaller mode were to be neglected in drawing the histographs of Figs. 10 and 12, the experimentally determined particle size distribution would be much closer to the calculated value.) We assert that the similarity in the particle size distributions is a stringent test of the match between experimental data and the theoretical calculations.

The results obtained from the experimental work and the theoretical model can be understood on the basis of a surface oxide layer, as suggested previously (*4*). Because of the volume difference between the oxide and the metal, a strain exists at the metal/oxide interface promoting particle splitting. A sufficiently small particle is converted entirely to oxide and no further splitting takes place (*5*). We suggest that both sintering and redispersion can occur during oxygen treatment. Some of the particles undergo *successive* splitting and are converted to smaller particles within the first 3 h of treatment. After this time, the smaller particles attain a limiting size, associated with their complete oxidation. They remain almost unaltered in size and number for the rest of the experiment. The other particles under a *net* sintering, leading to a net size increase, even though individual splitting/redispersion steps are not ruled out in the sequence. We expect that sintering occurs by adatom transfer between these larger particles; particle migration may occur as well. These larger particles have (at least) a layer of oxide on the surface, so that platinum oxide and alumina exist at the particle–support interface. The increased oxygen partial pressure associated with use of pure oxygen rather than air (as in the previous work) will promote oxide formation. However, the particle essentially is a platinum particle that undergoes sintering. The oxide–alumina interface results in a lower interfacial tension between the particle and the support, as indicated by the model from analysis of the experimental data.

Alternatively, the lowered interfacial tension may reflect stronger metal–support interaction made possible by greater support cleanliness arising from the added precautions taken to assure surface cleanliness in the present study.

Another view can also be proposed to understand the small particles. There must be some surface concentration of platinum adatoms. The model estimates a value of 2 μmol of platinum adatoms/m^2 of alumina, corresponding to 1.2 atoms/nm^2. Under the hard (10^{-8} Torr, ion-pumped) vacuum and the electron irradiation of the TEM, these adatoms might be "precipitated" as metal particles. The 2-nm circular particles seen by TEM could be taken as monolayer rafts or as four-layer hemispherical caps. Sweeping up all the adatoms in order to make the particles leads to a mean interparticle spacing of 6.8 nm for the rafts and 11.2 nm for the caps. As the large particles grow, the surface adatom concentration decreases so that the interparticle spacing grows. Such a rationale is consistent with the spacing of

the small particles in Figs. 7 and 9, although obviously needing further investigation.

SUMMARY AND CONCLUSIONS

Model platinum on alumina catalyst samples were prepared in the laboratory and sintered in purified, flowing oxygen at 600°C for 2, 3, 6, and 24 h. These materials were examined by ion scattering spectroscopy and transmission electron microscopy, where electron diffraction and X-ray emission spectroscopy as well as the recording of bright-field images were carried out.

The freshly prepared catalyst sample contains evenly distributed platinum particles of average size 4 nm. After 2 h of sintering, the average size increases, as expected. A few large particles are seen, along with many small ones. The size of the larger particles increases with sintering time to give an average of 20.9 nm after 6 h, and 29.7 nm after 24 h. The size distribution is distinctly bimodal, with a number of 2-nm particles evident after both treatments.

The theoretical model indicates that the interfacial tension between the particles and the support is lower for the present materials than that observed previously. An oxide film entirely covering the particles early in the experiment may be responsible. Some particles undergo successive splitting until they reach a limiting size, when they are completely oxidized. The large particles have at least a surface layer of oxide that lowers the interfacial tension between the particle and the support. However, the large particles behave essentially as platinum particles and undergo a net sintering among themselves, by transfer of adatoms, particle migration, or both.

APPENDIX: NOMENCLATURE

- C_p adatom concentration at the edge of a particle
- C_0 adatom concentration in equilibrium with an infinitely large particle (flat interface)
- k Boltzmann constant
- l_c characteristic length parameter
- R radius of a particle
- t time
- V_m molar volume of particle
- σ particle–substrate interfacial tension

ACKNOWLEDGMENTS

We are grateful to the National Science Foundation for support of the activity at West Virginia University under Grant CPE 83-20400. We are indebted to Dennis Swartzfager, Ronald Mattson, and William Lilly at du Pont for their assistance with ISS, TEM, and oxygen treatments, respectively.

REFERENCES

1. Ruckenstein, E., and Dadyburjor, D. B., *Rev. Chem. Eng.* **1,** 251 (1983).
2. Cocke, D. L., Johnson, E. D., and Merrill, R. P., *Catal. Rev. Sci. Eng.* **26,** 1 (1984).
3. Ruckenstein, E., and Malhotra, M. L., *J. Catal.* **41,** 303 (1976).
4. Gollob, R., and Dadyburjor, D. B., *J. Catal.* **68,** 473 (1981).
5. Dadyburjor, D. B., *in* "Catalyst Deactivation" (G. F. Froment and B. Delmon, Eds.). Elsevier, Amsterdam, 1980.
6. Dautzenberg, F. M., and Wolters, H. B. M., *J. Catal.* **51,** 26 (1978).
7. Sparrow, G. T., quoted in Brinen, J. S., D'Avignon, D. A., Myers, E. A., Deng, P. T., and Behnken, D. W., *Surf. Int. Anal.* **6,** 295 (1984).
8. Bellare, A., and Dadyburjor, D. B., *AIChE J.* **33,** 867 (1987).
9. Dadyburjor, D. B., Marsh, S. P., and Glicksman, M. E., *J. Catal.* **99,** 358 (1986).
10. Chakraverty, B. K., *J. Phys. Chem. Solids* **28,** 2401 (1967).